Hologram reconstruction using a digital micromirror device

Thomas Kreis, MEMBER SPIE
BIAS-Bremer Institut für angewandte Strahltechnik
Klagenfurter Str. 2
D 28359 Bremen, Germany
E-mail: thkreis@oskar.bias.uni-bremen.de

Petra Aswendt, MEMBER SPIE
Roland Höfling
IWU-Fraunhofer Institut für Werkzeugmaschinen und Umformtechnik
Reichenhainer Str. 88
D 09126 Chemnitz, Germany

Abstract. The aim of this work is an advancement of digital holographic interferometry by using a digital micromirror device (DMD) for real-time display of interferometric fringes. The theory describing the formation of the diffracted image produced by a coherently illuminated DMD is presented. Digital holograms of simple structures are calculated assuming plane and spherical reference waves, respectively. These synthetic holograms are used to control the micromirrors of the DMD, which now acts as a reflective hologram. Experimental holographic reconstructions of synthetic holograms prove the feasibility of DMDs in principle for this aim. Further experimental results show the reconstructed interferogram of fields recorded by digital holography and superposed numerically. This opens a new range of applications in digital holographic interferometry.
[DOI: 10.1117/1.1367346]

Subject terms: holography; digital holography; holographic interferometry; optical metrology; digital micromirror displays; computer-generated holograms; synthetic holograms.

Paper 200247 received June 22, 2000; revised manuscript received Dec. 29, 2000; accepted for publication Jan. 10, 2001.

1 Introduction

Holography is a method to record and to reconstruct entire optical wave fields, that is, intensity and phase, not only intensities as in photography. The method has found numerous applications, e.g. for display or in metrology. The combination of holography with computers and numerical techniques gave a strong boost to this coherent-optical method.[1] Computer-generated holograms allow the creation of wave fields that may be impossible to produce optically. Such wave fields are widely used in data storage, display, coherent image processing, and optical-component testing. Computer-aided holographic interferometry is a powerful method for measuring deformations, contours, or vibrations of opaque diffusely reflecting surfaces or the refractive index fields of transparent objects.[2] Digital holography now allows the recording of holograms with arrays of charge-coupled devices (CCDs) and performs the reconstruction of the complex wave fields numerically, thus enabling the comparison of the phase distributions of different object states in the computer.[3–5]

In a way computer-generated holography and digital holography are complementary. On the one hand the synthetic holograms are numerically generated, and are physically realized by a spatial light modulator (SLM) such as a positive-transparency film or a liquid crystal display (LCD). Then the wave field is reconstructed optically by illumination of the SLM with the reference wave.[6] On the other hand, in digital holography the holograms are optically generated, recorded by a CCD, and stored in a computer, and then the wave fields are reconstructed numerically. Both approaches face the same primary problem: the limited resolution of the SLMs and the CCDs.

Novel applications of digital holography and digital holographic interferometry include the superposition of previously recorded or numerically generated wavefields in actual wavefields in a sort of adaptive holographic interferometry, and the optical reconstruction of numerically superposed digital holograms to perform digital real-time hologram interferometry for vibrational or transient events. Although digital recording of holographic fields can be performed quickly, the digital reconstruction of the wavefields still takes about a minute (due to the numerically complex Fresnel transformation), and would require an optical reconstruction for real-time or quasi-real-time operation. The scheme of such an approach is shown in Fig. 1. Hologram recording is performed by a CCD array; the PC allows one to store and combine recorded holograms in an arbitrary manner. For the purpose of reconstruction an optical medium is necessary as the carrier of the hologram. Therefore we need an SLM that is fast, has large light throughput, and exhibits good diffraction efficiency.

This required performance is promised by one of the newest types of SLMs offered on the market today: the digital micromirror device (DMD*). The DMD was originally developed to be the core of a fully digital video display system.[7,8] It is a silicon micromachined component comprising an array of 16×16-μm tiltable aluminum mirrors mounted on hinges over a CMOS static random access memory (SRAM) chip. The mirrors are arrayed on a 17-μm pitch, providing a fill factor of nearly 90%. DMDs are commercially available in pixel counts of 640×480, 800×600, and 1280×1024.[9] Binary data sent to the DMD's

*DMD is a trademark of Texas Instruments Inc.

 0091-3286/2001/$15.00

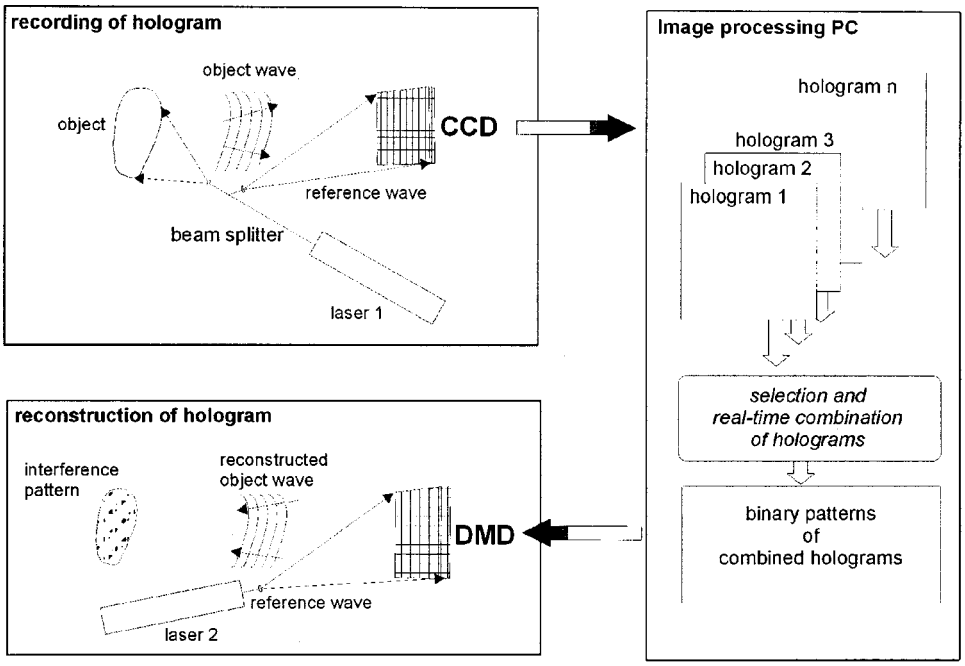

Fig. 1 Scheme of digital real-time hologram interferometry.

SRAM produce an electrostatic charge distribution, causing the individually addressed mirrors to tilt either −10 deg (on) or +10 deg (off) along an axis that is a diagonal of the micromirror.

While the LCD is a transmissive SLM absorbing up to 90% of the available light,[9] the DMD is a reflective one yielding much more light throughput. Furthermore, initial investigations have proven the superior diffraction efficiency of the DMD. These properties make the DMD promising for use as an SLM in reconstructing digital holograms. To our knowledge, up to now no efforts have been made to investigate the feasibility of DMDs for this aim. One interesting application of DMDs in holography is described by Nesbitt et al.,[9] where the DMD is used to display a series of two-dimensional stereoscopic perspective views that are being holographically recorded to generate a holographic stereogram. There the DMD produces the object wave in the recording step, and does not represent the hologram in the reconstruction step, as is our present intention. In this case[9] the hologram is still recorded on a standard silver halide plate.

Despite the good prospects concerning light throughput and diffraction efficiency, it is not clear initially that DMDs are usable to reconstruct holograms. One must address their limited resolution, their large pixel size, their fill factor less than 100%, and especially the motion of each micromirror, which may obstruct a useful holographic reconstruction.

Here we describe the results of the first investigations of DMDs used for optical reconstruction of digital holograms. The theory of image formation, which is closely related to the theory of digital holography, not only is used to explain the resulting images, but also constitutes the basis for calculating digital holograms. In first experiments calculated digital holograms have been used to control the DMD in order to generate the desired wave field when illuminated with the coherent reference wave. Furthermore, digital holograms have been recorded, and it was possible to reconstruct the sum hologram, providing the basis of the proposed digital real-time holographic interferometry.

2 Diffraction Field of a Coherently Illuminated DMD

If we try to use a DMD as a holographic structure, the first problem that arises is the limited resolution of the DMD. The pixel pitch dictates the maximum spatial frequency $f_{\max}$ that can be resolved. This is the same problem that had to be solved in digital holography when holograms were to be recorded on CCD arrays.[3–5] The maximum spatial frequency of the intensity variation in the hologram depends on the maximum angle $\theta_{\max}$ between the reference and the object wave:

$$f_{\max}=\frac{2}{\lambda}\sin\frac{\theta_{\max}}{2}. \tag{1}$$

Thus the DMD can resolve holographic structures as long as $\theta_{\max}$ remains small enough. This is the case if the object is of small size, or the object is far away from the hologram, or the wave field has been optically reduced. At the same time the reference wave must come from nearly the same direction as the object wave.[3–5]

Now let the DMD be illuminated by a monochromatic plane wave with unit amplitude impinging normally onto the micromirrors. The coordinates in the DMD plane are ξ, η. Then the optical field immediately in front of the DMD is given by[10]

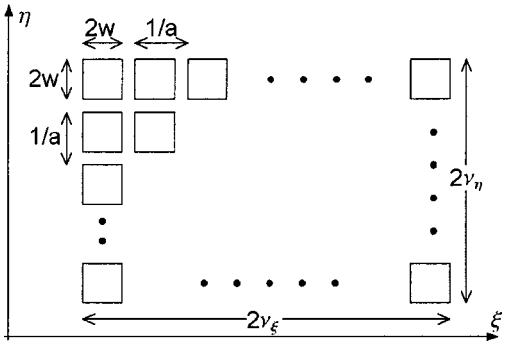

Fig. 2 Geometry of a digital micromirror display.

$$U(\xi,\eta)=\left\{\operatorname{rect}\left(\frac{\xi}{2w}\right)\operatorname{rect}\left(\frac{\eta}{2w}\right)\star\operatorname{comb}(a\xi)\operatorname{comb}(a\eta)\right\}\times\operatorname{rect}\left(\frac{\xi}{2v_\xi}\right)\operatorname{rect}\left(\frac{\eta}{2v_\eta}\right). \tag{2}$$

In this equation $\operatorname{rect}(\xi/2w)\operatorname{rect}(\eta/2w)$ describes the field reflected by a single square micromirror with side length $2w$ (Fig. 2). This is convolved ($\star$ symbolizing convolution) with the comb function $\operatorname{comb}(a\xi)\operatorname{comb}(a\eta)$, which represents the periodic replication of the micromirrors. The period of this replication is $1/a$. The convolution alone would represent an infinite number of micromirrors in each direction, but in fact we have only a finite number. Therefore the expression must be multiplied by $\operatorname{rect}(\xi/2v_\xi)\operatorname{rect}(\eta/2v_\eta)$, where $2v_\xi$ is the width of the whole DMD in the ξ direction, and $2v_\eta$ is the width in the η direction.

There are no mixed terms in Eq. (2), so we can separate it into two identical one-dimensional expressions

$$U(\xi,\eta)=U(\xi)U(\eta) \tag{3}$$

with

$$U(\xi)=\left\{\operatorname{rect}\left(\frac{\xi}{2w}\right)\star\operatorname{comb}(a\xi)\right\}\cdot\operatorname{rect}\left(\frac{\xi}{2v_\xi}\right). \tag{4}$$

The optical field $B(x,y)$ in the image plane at a distance d from the DMD is calculated from the Fresnel transform, which also can be separated:

$$B(x,y)=\frac{e^{ikd}}{ikd}\int_{-\infty}^{\infty}\int_{-\infty}^{\infty}U(\xi,\eta)\times\exp\left\{\frac{i\pi}{d\lambda}[(x-\xi)^2+(y-\eta)^2]\right\}d\xi\,d\eta=\frac{e^{ikd}}{ikd}I_\xi(x)I_\eta(y), \tag{5}$$

with

$$I_\xi(x)=\int_{-\infty}^{\infty}U(\xi)\exp\left[\frac{i\pi}{d\lambda}(x-\xi)^2\right]d\xi,\qquad I_\eta(y)=\int_{-\infty}^{\infty}U(\eta)\exp\left[\frac{i\pi}{d\lambda}(y-\eta)^2\right]d\eta. \tag{6}$$

Now it is sufficient to investigate $I_\xi(x)$; the result is also valid for the $I_\eta(y)$ in the other direction.

If we evaluate the squares and substitute $\mu=x/d\lambda$, we obtain

$$\begin{aligned}I_\xi(\mu)&=\exp(i\pi d\lambda\mu^2)\int_{-\infty}^{\infty}\left\{\operatorname{rect}\left(\frac{\xi}{2w}\right)\star\operatorname{comb}(a\xi)\right\}\times\operatorname{rect}\left(\frac{\xi}{2v_\xi}\right)\exp[(i\pi/d\lambda)\xi^2]\exp(-2i\pi\xi\mu)\,d\xi\\&=\exp(i\pi d\lambda\mu^2)\,\mathcal{F}\left\{\left[\operatorname{rect}\left(\frac{\xi}{2w}\right)\star\operatorname{comb}(a\xi)\right]\times\operatorname{rect}\left(\frac{\xi}{2v_\xi}\right)\exp[(i\pi/d\lambda)\xi^2]\right\},\end{aligned} \tag{7}$$

which represents a Fourier transform. Repeated application of the convolution theorem and use of the relations $\mathcal{F}\{\operatorname{rect}(\xi/2w)\}=2w\operatorname{sinc}(2w\mu)$ and $\mathcal{F}\{\operatorname{comb}(a\xi)\}=(1/a)\operatorname{comb}(\mu/a)$ yield

$$I_\xi(\mu)=\exp(i\pi d\lambda\mu^2)\left[2w\operatorname{sinc}(2w\mu)\frac{1}{a}\operatorname{comb}\left(\frac{\mu}{a}\right)\right]\star\mathcal{F}\left\{\operatorname{rect}\left(\frac{\xi}{2v_\xi}\right)\exp[(i\pi/d\lambda)\xi^2]\right\} \tag{8}$$

It remains to calculate the Fourier transform in Eq. (8)[10,11]:

$$\begin{aligned}&\mathcal{F}\left\{\operatorname{rect}\left(\frac{\xi}{2v_\xi}\right)\exp[(i\pi/d\lambda)\xi^2]\right\}\\&=\int_{-v_\xi}^{v_\xi}\exp\left(\frac{i\pi}{d\lambda}\xi^2\right)\exp(-2i\pi\xi\mu)\,d\xi\\&=\int_{-v_\xi}^{v_\xi}\exp\left[i\pi\left(\frac{\xi^2}{d\lambda}-2\xi\mu+d\lambda\mu^2\right)\right]\times\exp(-i\pi d\lambda\mu^2)\,d\xi\\&=\exp(-i\pi d\lambda\mu^2)\int_{-v_\xi}^{v_\xi}\exp\left[i\pi\left(\frac{\xi}{\sqrt{d\lambda}}-\sqrt{d\lambda}\mu\right)^2\right]d\xi.\end{aligned} \tag{9}$$

With $\alpha=\sqrt{2}\xi/\sqrt{d\lambda}-(2d\lambda)^{1/2}\mu$ the integral becomes a Fresnel integral, whose values are tabulated but also are contained in most modern computer software packages.

$$C(z)+iS(z)=\left(\frac{d\lambda}{2}\right)^{1/2}\int_{\alpha_1}^{\alpha_2}\exp\left(i\frac{\pi}{2}\alpha^2\right)d\alpha \tag{10}$$

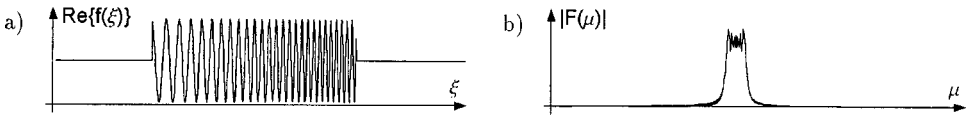

Fig. 3 Real part of the windowed chirp function and modulus of its Fourier transform.

with the integration limits

$$\alpha_1 = -\left(\frac{2}{d\lambda}\right)^{1/2} v_\xi - (2d\lambda)^{1/2}\mu,$$
$$\alpha_2 = +\left(\frac{2}{d\lambda}\right)^{1/2} v_\xi - (2d\lambda)^{1/2}\mu. \tag{11}$$

The corresponding Fresnel number is $N_F = v_\xi^2/d\lambda$, indicating that we are in the Fresnel region for the common parameters. This justifies the use of the Fresnel transform to calculate the free-space propagation. Altogether we obtain

$$\mathcal{F}\left\{\text{rect}\left(\frac{\xi}{2v_\xi}\right)\exp[(i\pi/d\lambda)\xi^2]\right\} = \left(\frac{d\lambda}{2}\right)^{1/2}\exp(-i\pi d\lambda\mu^2)\{[C(\alpha_2)-C(\alpha_1)] + i[S(\alpha_2)-S(\alpha_1)]\} \tag{12}$$

and

$$I_\xi(\mu) = \left(\frac{d\lambda}{2}\right)^{1/2}\left[\frac{2w}{a}\,\text{sinc}(2w\mu)\,\text{comb}\left(\frac{\mu}{a}\right)\right] \star\{[C(\alpha_2)-C(\alpha_1)] + i[S(\alpha_2)-S(\alpha_1)]\}. \tag{13}$$

The result of Eq. (12) is shown in Fig. 3. In Fig. 3(a) we see the real part of $\text{rect}(\xi/2v_\xi)\exp(i\pi\xi^2/d\lambda)$, and in Fig. 3(b) the modulus of its Fourier transform is given. We already met this distribution as the dc term of the Fresnel transform in digital holography.[12] Its intensity in two dimensions can roughly be interpreted as a rectangle. By the convolution in Eq. (13) this rectangle is replicated, where the period of the replication is given by the comb function as $ad\lambda$ in the x domain. The values of the intensities of the replicas, up to a constant factor, are governed by the sinc-function values at the teeth of the comb. The highest intensity is at $\mu = 0$. But here we have to notice the interesting fact that the higher-order replicas do not vary strongly at consecutive orders for the special choice of mirror width $2w = 16\,\mu$m and a pitch of 17 μm. This is shown in Fig. 4(a), where the values of $|\text{sinc}[16\mu]|$ at the points where $\text{comb}[17\mu]$ is nonzero are emphasized. For a hypothetic mirror width of $2w = 14\,\mu$m and the pitch 17 μm, there would be more variation; this case is displayed in Fig. 4(b).

After this preparation we can calculate the intensity in the Fresnel region, Fig. 5(b), when a series of mirrors, here 30 mirrors of width 16 μm with pitch 17 μm [Fig. 5(a)], is given. Although in the one-dimensional simulation only 30 mirrors instead of the 800 in the real DMD were used, the calculated result resembles exactly the situation when the physical DMD with each micromirror at rest is illuminated by a plane wave of coherent laser light.

A further test confirming the above theory and preparing for the application of DMDs for reconstructing digital holograms is when each second mirror is flipped and does not reflect in the investigated direction. The results of this simulation are shown in Fig. 6. The calculated Fresnel field again coincides with the experimentally produced image field. Halving the number of mirrors in the spatial domain corresponds to doubling the number of peaks in the spatial-frequency domain. Such experiments have been carried out using a DMD, and the results confirm the theoretical modeling [Fig. 5(c), 6(c)]. In addition, the validity of the DMD model has been verified by checking the influence of the $\pm$10-deg tilt. It can be shown that this will introduce a multiplication by $\exp[2\pi\xi\sin(10\text{deg})/\lambda]$, representing a tilted illumination wave. This modification has no effect on the main results shown above.

3 Calculation of Synthetic Holograms

In Sec. 2 we have shown theoretically—and also confirmed experimentally—that the periodic structure and the fill factor less than 100% of the DMD lead to a replication of the diffracted pattern when the DMD reflects coherent illumination. Thus we can expect to be able to use the DMD as a binary reflection hologram where the holographic structure is defined by the micromirrors flipped into (+10 deg) and flipped out of (−10 deg) the reflection direction, or vice versa.

Let the wave field whose hologram has to be calculated be given in the (x,y) plane, the object plane, by

$$b(x,y) = |b(x,y)|\exp[i\beta(x,y)]. \tag{14}$$

The hologram is determined at the distance d from the object plane. The field in the hologram plane is calculated from the Fresnel transform

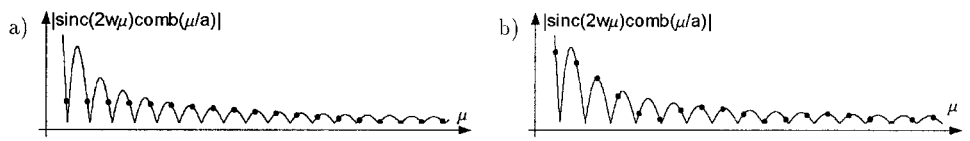

Fig. 4 Values of $|\text{sinc}(2w\mu)\text{comb}(\mu/a)|$ for $1/a = 17$ and (a) $2w = 16$, (b) $2w = 14$.

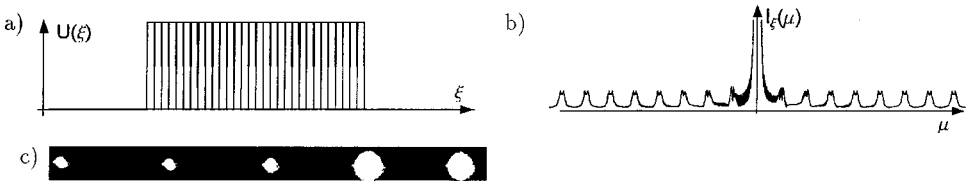

Fig. 5 (a) Reflectivity of a series of mirrors, and (b) its Fresnel field.

$$\Gamma(\xi,\eta)=\int\int b(x,y)\exp\left[i\pi\frac{(x-\xi)^2+(y-\eta)^2}{d\lambda}\right]\mathrm{d}x\,\mathrm{d}y, \tag{15}$$

which after evaluation of the squares in the exponential and with the substitutions $\mu=\xi/(d\lambda)$ and $\nu=\eta/(d\lambda)$ is

$$\Gamma(\mu,\nu)=\exp[i\pi d\lambda(\mu^2+\nu^2)]\int\int b(x,y)\times\exp\left[\frac{i\pi}{d\lambda}(x^2+y^2)\right]\times\exp[-2i\pi(x\mu+y\nu)]\,\mathrm{d}x\,\mathrm{d}y. \tag{16}$$

Its discrete finite version, which is used for the numerics, is

$$\Gamma(m\,\Delta\xi,n\,\Delta\eta)=\exp\left[\frac{i\pi}{d\lambda}(m^2\,\Delta\xi^2+n^2\,\Delta\eta^2)\right]\times\sum_{k=0}^{M-1}\sum_{l=0}^{N-1}b(k\,\Delta x,l\,\Delta y)\times\exp\left\{i\pi d\lambda\left[\frac{k^2}{(M\,\Delta\xi)^2}+\frac{l^2}{(N\,\Delta\eta)^2}\right]\right\}\times\exp\left[-2i\pi\left(\frac{km}{M}+\frac{ln}{N}\right)\right] \tag{17}$$

with $\Delta x=1/(M\,\Delta\mu)=d\lambda/(M\,\Delta\xi)$, $\Delta y=1/(N\,\Delta\nu)=d\lambda/(N\,\Delta\eta)$, $\Delta\xi$ and $\Delta\eta$ the pixel pitch in the corresponding directions, and λ the wavelength of the laser light to be used for reconstruction. The double sum in Eq. (17) represents a two-dimensional Fourier transform and is easily calculated by the FFT algorithm. Thus we have the complex wave field in the hologram plane. The final synthetic hologram $h(m\,\Delta\xi,n\,\Delta\eta)$ we obtain by adding the intended reconstruction wave $r(m\,\Delta\xi,n\,\Delta\eta)$ to the field $\Gamma(m\,\Delta\xi,n\,\Delta\eta)$ and taking the squared modulus:

$$h(m\,\Delta\xi,n\,\Delta\eta)=|\Gamma(m\,\Delta\xi,n\,\Delta\eta)+r(m\,\Delta\xi,n\,\Delta\eta)|^2. \tag{18}$$

In contrast with the numerical reconstruction of digital holograms in digital holography, we cannot neglect the phase factor preceding the double sum, because $|\Gamma+r|^2\neq|e^{i\alpha}\Gamma+r|^2$ for $\alpha\neq n\,2\pi$, $n\in\mathbb{N}$, as can easily be shown. The hologram h now consists of $M\times N$ floating-point values, which are quantized to binary data, black or white, corresponding to micromirrors flipped in or flipped out. For the FFT calculation, M and N should be powers of 2; here we had $M=N=1024$. For the control of the DMD the central 800×600 values are taken from the binary 1024×1024 value field. The pixel periods have to be taken as $\Delta\xi=\Delta\eta=17\,\mu$m, and since a He-Ne laser is used for reconstruction, $\lambda=0.6328\,\mu$m.

In the performed experiments the object was a circular ring [Fig. 7(a)] with

$$|b(x,y)|=\begin{cases}1 & (x,y)\in\text{ring}\\ 0 & \text{outside}\end{cases}, \tag{19}$$

and $\beta(x,y)$ stochastically varying between 0 and 2π; the latter is calculated by a suitable random generator subroutine. The binary hologram of this object field at a distance $d=1.0$ m looks like Fig. 7(b), which displays roughly a quarter of the total synthetic hologram. The reference wave can be arbitrary: it may be a plane wave, but this would result in relatively large replicated dc terms in the reconstructed image. Better suited is a convergent reference wave, which also was used in preparing the hologram of Fig. 7(b).

4 Experimental Results

Experiments were carried out to verify the theoretical predictions using a Texas Instruments DMD with 800×600 micromirrors (SVGA) arranged on a $13.6\times10.2\,\mathrm{mm}^2$ area. The DMD is part of an ODS 800 projection system[13] designed for optical metrology; this device provides free access to the DMD chip. Two types of reference wave have been realized, as shown in the optical layouts of Figs. 8 and 9. These figures indicate the positions of the central dc

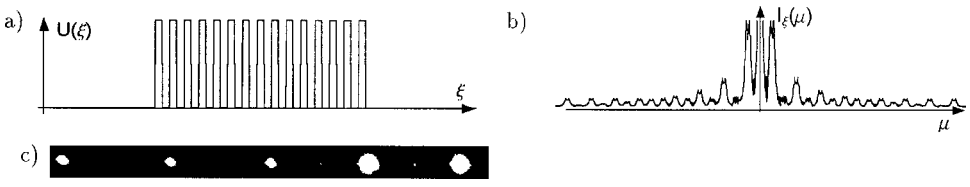

Fig. 6 (a) Reflectivity of a series of mirrors, and (b) its Fresnel field.

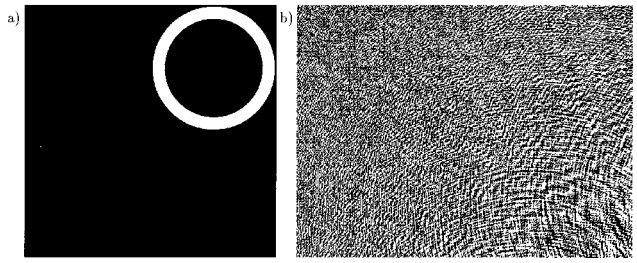

Fig. 7 Artificial object (a) and part of its synthetic binary hologram (b).

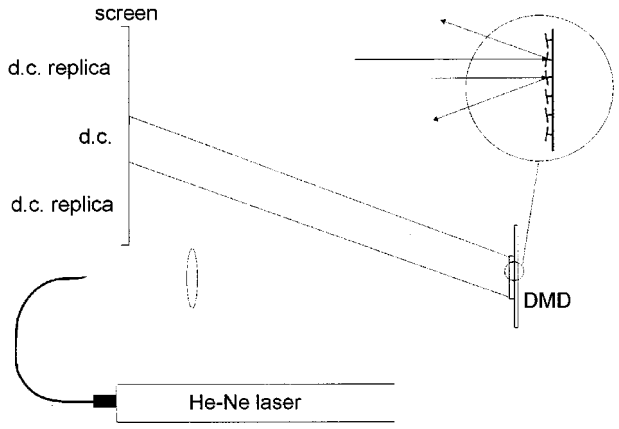

Fig. 8 Optical layout: plane wave.

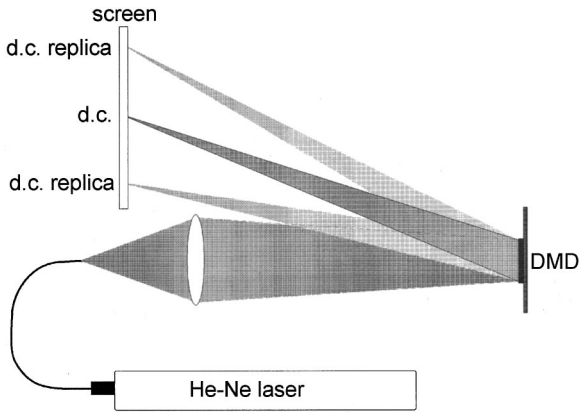

Fig. 9 Optical layout: convergent wave.

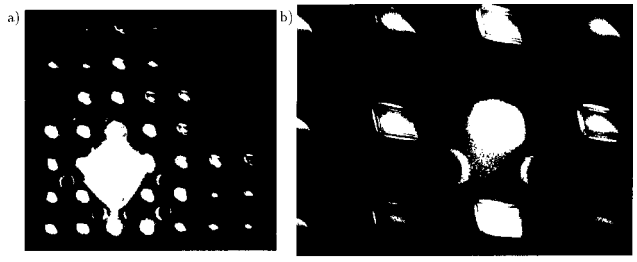

Fig. 10 Reconstructed real image (a) and detail (b) for plane reference wave.

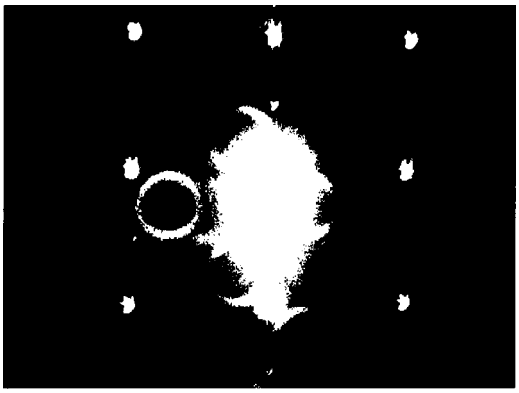

Fig. 11 Reconstructed image for convergent reference wave.

component and the periodic replication of this term. The reconstructed real images of the object are placed between these replicas.

The DMD is computer-controlled by the output channel of a Matrox Pulsar imaging board, and special software has been written to load the digital holograms into the DMD. A 30-mW He-Ne laser is used to reconstruct the holograms. The laser light is fed into a single-mode optical fiber, and an objective lens creates either a plane or a converging wave, illuminating the DMD at normal incidence. According to the 10-deg tilt of the micromirrors, the direct light (zero order of diffraction) is deflected by 20 deg. A white screen was placed 1 m away from the DMD to visualize the real image of the holographic reconstruction.

In the case of the collimated beam (plane reference wave), the bright rectangular spot in the central lobe of the diffraction pattern represents the dc term and resembles a picture of the DMD itself. This dc spot is surrounded by a number of equally spaced replicas, as seen in the example of Fig. 10. Here the synthetic binary hologram of Fig. 7 has been loaded into the DMD, and the corresponding circles are reconstructed between the repeated dc spots. The theoretical predictions are completely confirmed: the real images are reconstructed at 1-m distance from the DMD. The virtual images are defocused in this plane and therefore not visible; they just produce a background intensity variation.

The second optical arrangement, Fig. 9, has a strong practical advantage. The use of a reference wave converging in the plane of the object or of a real image allows suppressing the dc spots significantly. This layout is equivalent to lensless Fourier holography. Both real and virtual images are expected to focus in the plane of the screen. Figure 11 shows the experimental result when a synthetic hologram, calculated with a spherical reference wave, is loaded into the DMD and is illuminated by the converging beam. The dc patterns are concentrated now in small spots, and two circles, one real and one virtual image, are reconstructed with any dc replica.

In a further experiment a digitally recorded hologram of a real object was taken for reconstruction by DMD. An aluminum plate was illuminated by an argon ion laser with wavelength 0.5145 μm, and the hologram was produced using a plane reference wave. The CCD target had 1024 $\times$1024 pixels of size 6.8$\times$6.8 μm with 100% fill factor. The recorded digital hologram was reduced from 256 gray

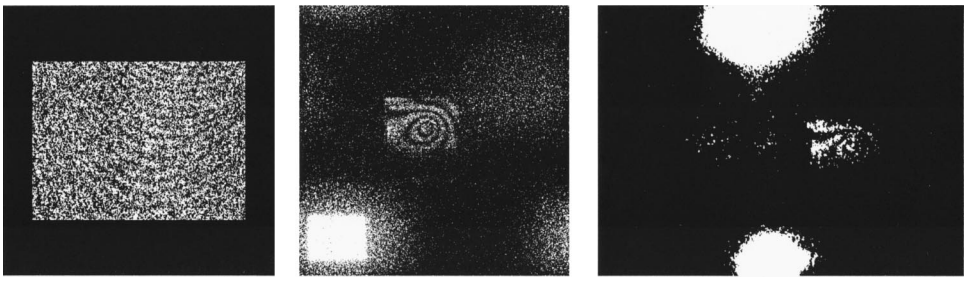

Fig. 12 Example of digital holographic interferometry. Left: sum of holograms; middle: numerical reconstruction; right: DMD reconstruction.

values to a binary hologram and restricted to the central 600×800 pixels. The difference in the pixel size of CCD and DMD, as well as the variation of wavelength from recording with $\lambda_{CCD}=0.5145\,\mu$m to reconstruction with $\lambda_{DMD}=0.59104\,\mu$m led to a modification of the distance where the real image is found. If the recording distance between object and CCD is d and if $\Delta\xi_{CCD}=\Delta\eta_{CCD}$ and $\Delta\xi_{DMD}=\Delta\eta_{DMD}$, then the reconstruction distance d' between DMD and real image is given by

$$d'=d\frac{\Delta\xi_{DMD}\cdot\lambda_{CCD}}{\Delta\xi_{CCD}\cdot\lambda_{DMD}}. \tag{20}$$

In the experiment performed the plate was $d=0.33$ m away from the CCD, so the real image can be expected at the distance $d'=0.718$ m.

The final aim is to use DMD reconstruction for metrologic tasks employing digital holographic interferometry. Therefore a second digital hologram of the now loaded aluminum plate was recorded. The pointwise sum of the two holograms then was binarized and fed to the DMD. Figure 12 shows the experimental result in comparison with the numerical reconstruction. Using the same input data (Fig. 12, left), the interference fringes appear in the real image, and a very good correspondence is found between the optical and the numerical reconstruction. A closer view is given in Fig. 13. The aluminum plate is seen with and without load, and the resulting interferogram of the two states can be clearly observed as well. This result confirms the feasibility of the intended real-time technique of digital holography. The DMD with its 17-μm pitch proved well suited as the carrier of an amplitude hologram. Interference fringes can be observed from double-exposure holograms combined by the controlling PC.

5 Conclusions and Outlook

In the present paper we have described the fundamentals of wavefield reconstruction by illuminating a DMD with coherent light, where the micromirrors of the DMD are controlled by a binary digital hologram. The basic theory used for calculating the digital hologram of the desired wavefield, as well as for simulating numerically the wavefield resulting from illumination of the DMD, is given. First experiments have proved this approach. Thus we have shown successfully not only the feasibility of hologram reconstruction by DMDs but also their applicability in holographic interferometric metrology.

There still remain some questions: In principle we are not restricted to binary holograms, but may reflect gray values by pulse width modulation (PWM) of the flipping of the mirrors. For this approach, which is still a binary one, it must be guaranteed that there is enough temporal overlap of the micromirrors flipped into the reflecting state to enable the coherent superposition of the elementary spherical waves according to Huygens's theory. Further, we have to design an optical arrangement that masks out and magnifies a single one of the replicated reconstructions. A possible application is in digital holographic interferometry: The numerical addition of a stored and an actual digital hologram can be performed in nearly real time; the resulting sum hologram can be reconstructed by the DMD. In this way real-time digital holography can be realized. It is also imaginable that the DMD-reconstructed wavefield might be superposed to an optically generated one for interferometric measurements. The preliminaries and theoretical tools for solving these problems are given above.

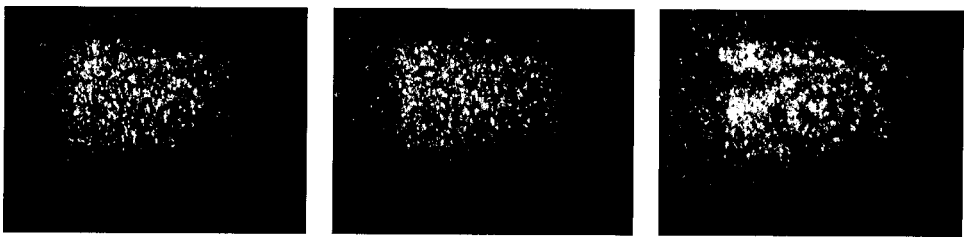

Fig. 13 DMD reconstruction of an Al plate. Left: initial state; middle: loaded state; right: holographic interferogram.

Acknowledgments

The described research was sponsored by the German Research Council (Deutsche Forschungsgemeinschaft DFG) under grants Kr 953/16 and Ho 1606/3. This support is gratefully acknowledged.

References

1. T. Kreis, ''Computer-aided evaluation of holographic interferograms,'' in *Holographic Interferometry*, P. K. Rastogi, Ed., Springer Series in Optical Sciences, Vol. 68, pp. 151–212 (1994).
2. T. Kreis, *Holographic Interferometry: Principles and Methods*, Wiley-VCH, New York, Weinheim (1996).
3. U. Schnars, ''Direct phase determination in hologram interferometry with use of digitally recorded holograms,'' *J. Opt. Soc. Am. A* **11**, 2011–2015 (1994).
4. U. Schnars, T. M. Kreis, and W. P. O. Jüptner, ''Digital recording and numerical reconstruction of holograms: reduction of the spatial frequency spectrum,'' *Opt. Eng.* **35**(4), 977–982 (1996).
5. T. Kreis, W. Jüptner, and J. Geldmacher, ''Digital holography: methods and applications,'' in *Int. Conf. on Applied Optical Metrology, Proc. SPIE* **3407**, 169–177 (1998).
6. S. Krüger, J. Kamps, and G. Wernicke, ''Spatial light modulator system for the application as dynamic diffractive element and in optical image processing,'' *Proc. SPIE* **3951**, 179–190 (2000).
7. R. J. Gove, ''DMD display systems: the impact of an all-digital display,'' in *Int. Symp. Society for Information Display*, Texas Instruments White Pages, http://www.ti.com//dlp/docs/developer/resources/white/index.shtml (1994).
8. L. J. Hornbeck, ''Digital light processing update: status and future applications,'' in *Conf. on Projection Displays V, Proc. SPIE* **3634**, 158–170 (1999).
9. R. S. Nesbitt, S. L. Smith, R. A. Molnar, and S. A. Benton, ''Holographic recording using a digital micromirror device,'' in *Conf. on Practical Holography XIII, Proc. SPIE* **3637**, 12–20 (1999).
10. J. W. Goodman, *Introduction to Fourier Optics*, 2nd ed., McGraw-Hill, New York, 1996.
11. A. Papoulis, *Signal Analysis*, int. student ed., McGraw-Hill, 1977.
12. T. Kreis and W. Jüptner, ''The suppression of the dc term in digital holography,'' *Opt. Eng.* **36**, 2357–2360 (1997).
13. G. Frankowski, ''The ODS 800—a new projection unit for optical metrology,'' in *Fringe '97—Automatic Processing of Fringe Patterns*, pp. 533–539, Akademie-Verlag, Berlin, and VCH, New York (1997).

Thomas Kreis received his diploma in mathematics from the University of Göttingen. He spent three years as a research assistant at the Institute for Metrology in Engineering, University of Hanover, where he obtained his PhD in mechanical engineering. He joined the Bremer Institut für angewandte Strahltechnik (the Bremen Institute for Applied Beam Technology) in 1980, where he was first responsible for the field of fundamentals and data processing and since 1986 has headed the Department of Laser Metrology. His research activities range from mathematical methods in optics and laser applications to image processing and coherent optical metrology. His main interest is in computer-aided holographic interferometry. Dr. Kreis is the 1987 recipient of the Hans-Rottenkolber Award for outstanding contributions in laser-assisted metrology. He is a member of SPIE, OSA, and DGaO.

Petra Aswendt received her MS degree in materials science from the Freiberg Mining Academy in 1982. She joined the Institute of Mechanics in the same year. There, she was engaged in experimental mechanics of materials with emphasis on holographic interferometry and speckle techniques. She continued work in this field at the Fraunhofer Institute IWU in Chemnitz, where she is currently the head of the Micrometrology Group. She received her PhD from the Dortmund University of Technology in 1995. She has published more than 25 papers focused on the application of optical metrology in experimental mechanics and nondestructive testing.

Roland Höfling received his MS degree in physics from the Dresden University of Technology in 1979. After five years work in the software industry, he joined the Institute of Mechanics in Chemnitz. His scientific work concentrated on digital image processing in optical metrology. In 1988, he received his PhD degree in physics from the Chemnitz University of Technology. Since 1991 he has been working in the Fraunhofer Institute IWU in Chemnitz, where he is currently the head of the Microfabrication Center. He has numerous publications in journals and conference papers in the field of optical metrology. He is chair of the Holographic Interferometry and Speckle Techniques working group within the German society VDI/VDE-GESA, as well as a member of SPIE.